

Catalysis

Sterically Demanding Ag⁺ and Cu⁺ N-Heterocyclic Carbene Complexes: Synthesis, Structures, Steric Parameters, and Catalytic Activity

Alejandro Cervantes-Reyes,^[a] Frank Rominger,^{†, [a]} and A. Stephen K. Hashmi*,^[a, b]

Abstract: The synthesis and full characterization of new air-stable Ag⁺ and Cu⁺ complexes bearing structurally bulky expanded-ring N-heterocyclic carbene (erNHC) ligands is presented. The condensation of protonated NHC salts with Ag₂O afforded a collection of Ag⁺ complexes, and their first use as ligand transfer reagents led to novel isostructural Cu⁺ or Au⁺ complexes. In situ deprotonation of the NHC salts in the presence of a copper(I) source, provides a library of new Cu⁺ complexes. The solid-state structures feature large *N*-C_{NHC}-N angles (118–128°) and almost identical angles between the aryl groups on the nitrogen atoms and the plane

of the *N*-C-N unit of the carbene (i.e. torsion angles close to 0°). Among the steric parameters, the percent buried volume (%V_{bur}) values span easily in the 50–57% range, and that one of (9-Dipp)CuBr complex (%V_{bur}=57.5) overcomes to other known erNHC–metal complexes reported to date. Preliminary catalytic experiments in the copper-catalyzed coupling between *N*-tosylhydrazone and phenylacetylene, afforded 76–93% product at the 0.5–2.5 mol % catalyst loading, proving the stability of Cu⁺ erNHC complexes at elevated temperatures (100 °C).

Introduction

Pioneering work of by Wanzlick in the early 60's inaugurated the era of N-heterocyclic carbenes (NHCs) as ligands for metals.^[1] Thereafter, new breakthroughs achieved by Arduengo, Bertrand, and Herrmann, led to the application of NHCs in organometallic chemistry and catalysis.^[2–4] Since then, NHC ligands are considered excellent candidates for the stabilization of a wide range of metal complexes,^[5] and particularly for the ubiquitous coinage metals (Ag, Cu, Au),^[6] thanks to their strong σ-donating ability and steric properties.^[7]

N-heterocyclic carbenes based on expanded-ring backbone^[8] have emerged as outstanding ligands for transition-metal complexes,^[9] as a result of the enlarged *N*-C_{NHC}-N angle that pushes the N-substituent closer to the carbene carbon providing steric protection around the metal center and consequently, enhanc-

ing the final catalytic activity of the complex.^[10–11] Furthermore, the trend to increase the steric demand of the ligand, has strongly influenced the field of catalyst design.^[7,8,10] For instance, by tuning the substituent on the *N*-atom in the tether^[12] or the backbone of the NHC skeleton,^[13] a unique class of structurally imposing metal complexes has arisen (%V_{bur}>52).^[14]

For several years, Ag⁺ NHC complexes have been fruitfully explored in medicinal chemistry as biologically active organometallic complexes,^[15] joining a swift application in catalysis.^[16] Owing to the low thermodynamic stability of the carbene carbon–silver bond, Ag⁺ NHC complexes are also useful synthetic reagents in ligand transfer reactions,^[17] becoming a convenient entry point into other NHC–metal compounds.^[13c,18] On the other hand, many NHC-stabilized Cu⁺ complexes are key catalysts of synthetically relevant transformations,^[19] and during the last decade, became a „hot topic“ thanks to their photophysical properties.^[20]

Although manifold examples of Ag⁺ and Cu⁺ complexes bearing erNHC ligands have been developed,^[18b,21] their structural diversity is limited by a flexible alkyl-chain design, which lead to a poor prediction of their structural features, as the ring geometry affects the NHC complex sterics and electronics.^[5i, 9i, 13a] The steric bulkiness of several erNHC metal complexes generally overcomes that of the imidazolylidene-containing ligands (i.e. IPr) albeit rarely surpass the „latest generation“ five-membered NHCs such as IPr** or IPr*(^{2–Np}) (Figure 1).

[a] A. Cervantes-Reyes, Dr. F. Rominger,[†] Prof. Dr. A. S. K. Hashmi
Organisch-Chemisches Institut, Heidelberg University
Im Neuenheimer Feld 270, 69120 Heidelberg (Germany)
E-mail: hashmi@hashmi.de

[b] Prof. Dr. A. S. K. Hashmi
Chemistry Department, Faculty of Science
King Abdulaziz University, Jeddah 21589 (Saudi Arabia)

[†] Crystallographic investigation

 Supporting information and the ORCID identification number(s) for the author(s) of this article can be found under:
 https://doi.org/10.1002/chem.202000600.

 © 2020 The Authors. Published by Wiley-VCH Verlag GmbH & Co. KGaA.
This is an open access article under the terms of Creative Commons Attribution NonCommercial-NoDerivs License, which permits use and distribution in any medium, provided the original work is properly cited, the use is non-commercial and no modifications or adaptations are made.

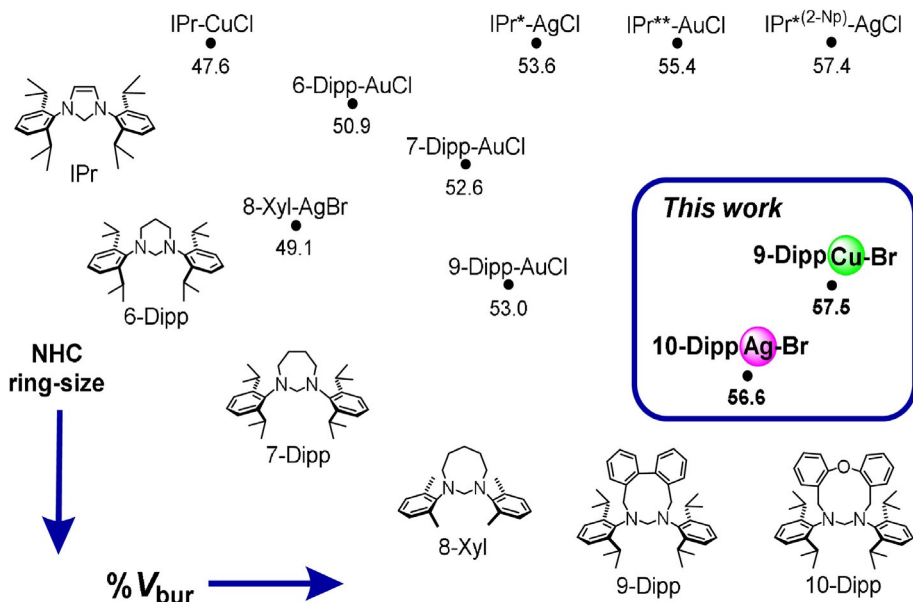


Figure 1. Selected complexes of Ag^{I} , Cu^{I} and Au^{I} complexes stabilized by five- to 10-membered NHC ligands.

Results and Discussion

Protonated BF_4^- (**1a**) and PF_6^- (**1b**) salts shown in Figure 2, served as ligand source for the synthesis of Ag^{I} and Cu^{I} erNHC complexes. Ligands 9-Dipp, 9-Mes, 9-Dietph, 9-Xyl, 10-Dipp, 10-Mes, 10-Dietph and 10-Xyl are relatively unexplored in metal complex synthesis so far.^[14]

The BF_4^- salts **1aa–1ah** were easily accessible by our previously reported procedure.^[14] The reaction of erNHC-HBr precursors with NH_4PF_6 in MeOH at room temperature, originated their hexafluorophosphate analogues **1ba–1bh**. Anion exchange was confirmed via ^1H , ^{31}P and ^{19}F NMR analysis. The amidinium protons were evidenced in the ^1H NMR spectra by the characteristic singlet signal at δ 7.5–8.0 ppm, while the ^{31}P NMR displayed a septet signal at ca. δ –144 ppm, in the typical range for hexafluorophosphate derivatives. The structure of PF_6 salt **1ba** was unambiguously confirmed by a single crystal X-ray diffraction analysis (Figure S2, see the Supporting Information).^[22]

Ag^{I} and Cu^{I} NHC complexes

The reaction of protonated NHC salts and Ag_2O to erNHC- AgX complexes has been studied in great detail.^[17,23] This reaction proceeds better with weakly coordinating anions (e.g. BF_4^- or PF_6^-) rather than halides (e.g. Br^- , Cl^- , I^-), presumably due to the halide counter anion is being able to form an hydrogen bond with the C2-H amidinium proton.^[5e,21c] Hence, the optimization experiments employing the erNHC salts of bulky ligands 9-Dipp and 10-Dipp were conducted (Table 1). Satisfyingly, the formation of Ag^{I} erNHC complexes was observed in all cases.

The screening in CH_2Cl_2 at room temperature (Entries 1 and 2) led to the expected products in poor yields (17 and 21%, respectively) after 24 h. The total consumption of the substrate required a longer reaction time (ca. 3 days) yielding <50%

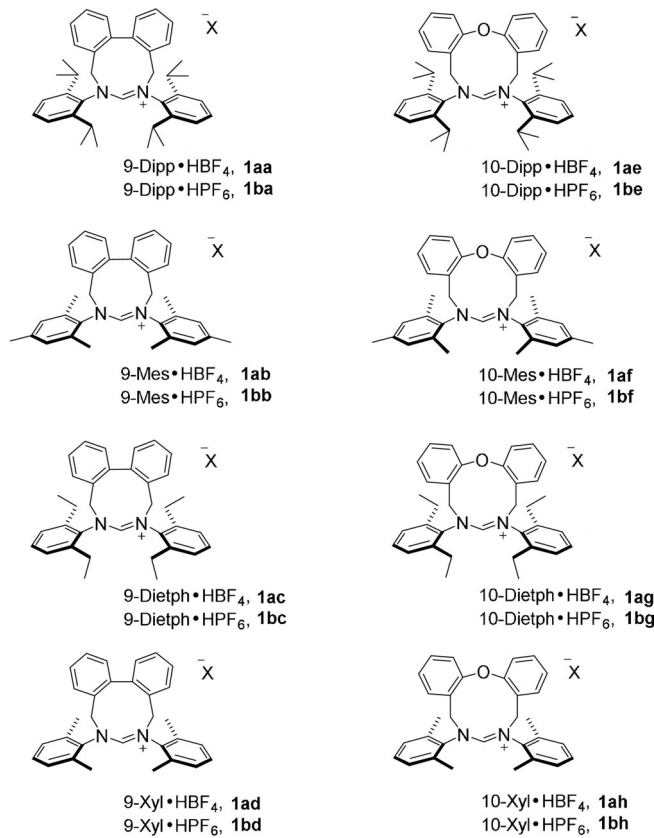


Figure 2. Protonated erNHC salts employed in this study (Dipp = 2,6-diisopropylphenyl, Mes = 2,4,6-trimethylphenyl, Dietph = 2,6-diethylphenyl and Xyl = 2,6-dimethylphenyl).

product. The reaction also was effective in CH_3CN under heating conditions (Entries 3 and 4), where the yields raised up to 54%. By using THF as the solvent and higher temperature (68°C), the yields enhanced notably (>70%, Entries 5 and 6) as

Table 1. Optimization of the synthesis of Ag^I erNHC complexes.

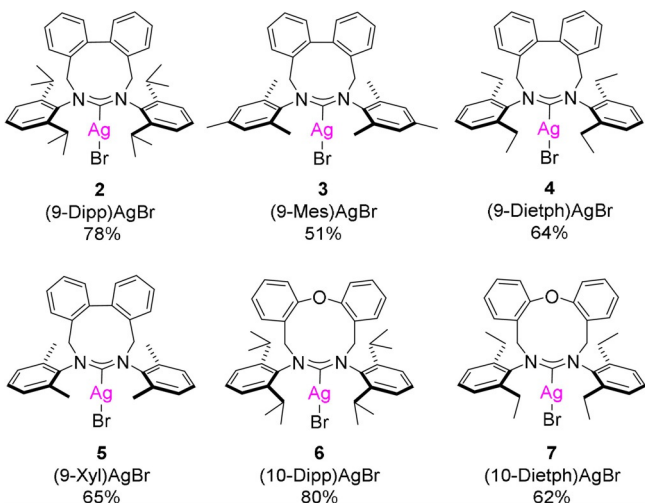
| Entry | Substrate | Conditions ^[a] | Product | Yield [%] ^[b] | Y = none, 2 |
|-------|-------------|--|----------|--------------------------|--------------------|
| | | | | | Y = O, 6 |
| 1 | 1 aa | CH ₂ Cl ₂ , r.t. | 2 | 17 | |
| 2 | 1 ae | | 6 | 21 | |
| 3 | 1 aa | CH ₃ CN, 50 °C | 2 | 48 | |
| 4 | 1 ae | | 6 | 54 | |
| 5 | 1 aa | | 2 | 75 | |
| 6 | 1 ae | THF, 68 °C | 6 | 80 | |
| 7 | 1 ba | | 2 | 41 | |

[a] Reaction conditions: NHC-HBF₄ (0.1 mmol, 1.0 equiv), Ag₂O (0.1 mmol, 1.0 equiv), NaBr (0.6 mmol, 6.0 equiv), absolute solvent (3 mL), in dark, 24 h. [b] Isolated yields as an average of two runs.

a result of a better solubility of substrate and Ag₂O, leading to a full consumption (revealed by TLC, CH₂Cl₂ 100%). Interestingly, the use of salt **1 ba** under same reaction conditions, diminished the yield to a half, and most substrate remained unreacted (Entry 7).

While attempting the synthesis of **4** from **1 ac** and Ag₂O in THF at reflux for 3 days, organic material was isolated as the main product and further identified as the ring opened NHC **1 ac'** (formed presumably as a result of hydrolysis with water catalyzed by heating). A sample of this material crystallized from a toluene solution after several days and the X-ray diffraction analysis of a single crystal confirmed its composition and structure (**1 ac'**, Figure S3, see the Supporting Information).^[22]

Finally, the reaction of various BF₄⁻ salts with Ag₂O and NaBr in THF under reflux for 24 h, provides a collection of Ag^I erNHC complexes in acceptable to good yields (51–80%, Figure 3). Complexes **2–7** are air- and moisture-stable, colorless solids

**Figure 3.** Ag^I complexes **2–7** bearing erNHC ligands.

and after recrystallization from a CH₂Cl₂:pentane mixture, high purity crystalline solids can be obtained.

Unfortunately, the isolation of Ag^I complexes bearing 10-Mes or 10-Xyl ligands was unsuccessful. Under these reaction conditions, decomposition material was observed instead.

Spectroscopic characterization of Ag^I erNHC complexes **2–7** by ¹³C{¹H} NMR reveals the typical carbene carbon (C_{NHC}) signals of two doublets displaced in high chemical shifts with coupling constants of $^1J_{C^{107}\text{Ag}}=224\text{--}227\text{ Hz}$, and $^1J_{C^{109}\text{Ag}}=260\text{--}263\text{ Hz}$, in agreement with the spin–spin interaction between ¹⁰⁷Ag (spin $\frac{1}{2}$, 51.8%) and ¹⁰⁹Ag (spin $\frac{1}{2}$, 48.2%) isotopes with the singlet C_{NHC}.^[21c] The ratio of these constants reflects approximately the gyromagnetic ratio γ for the two silver nuclei involved that is $\gamma(^{109}\text{Ag})/\gamma(^{107}\text{Ag})=1.15$.^[24]

These observed couplings indicate a relatively strong C_{NHC}–Ag bond as a result of no or slow exchange of the erNHC ligands between the Ag atoms at the NMR scale^[13b] and confirms that complexes **2–7** do not exhibit a fluxional behavior in the C_{NHC}–Ag bond, characterized by the lack of C_{NHC}–Ag couplings.^[17]

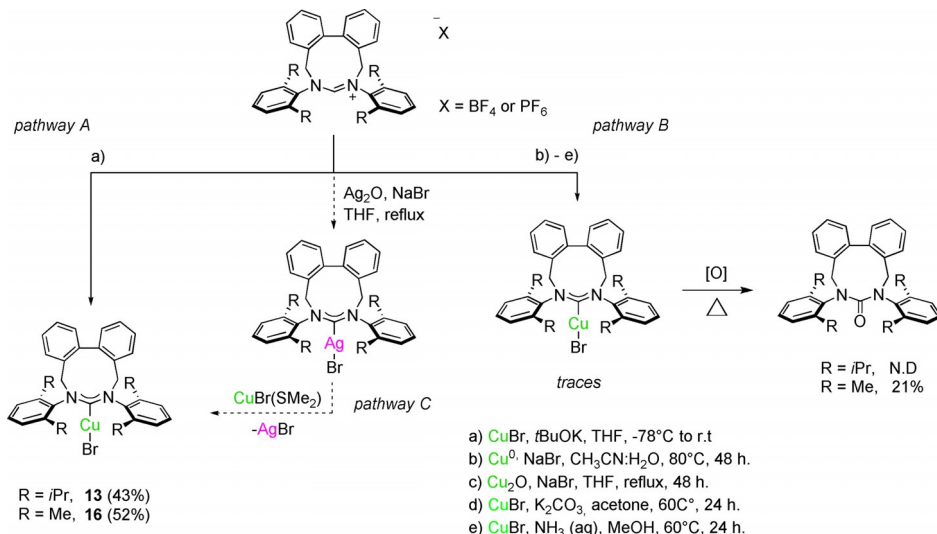
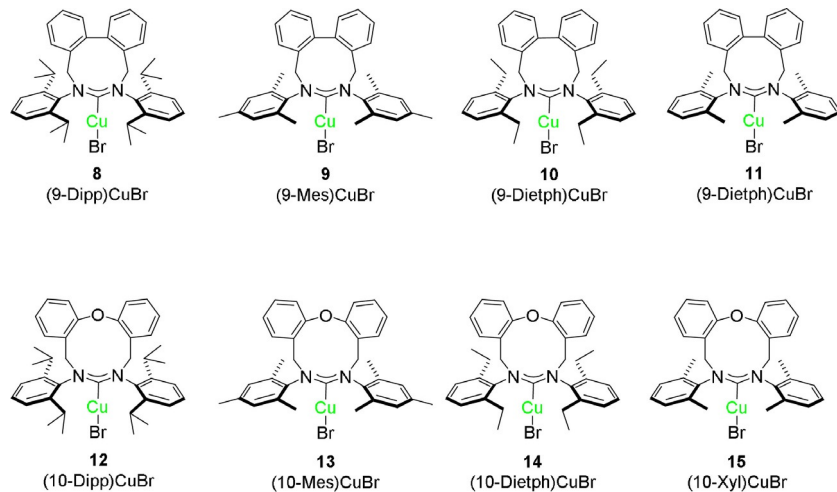
Mass spectrometry analyses (MALDI, ESI+) proved the [(erNHC-Ag)₂Br]⁺, [(erNHC)₂-Ag]⁺ and [(erNHC-Ag)₂]⁺ fragments but commonly, the most prominent peak in the spectra is that of the [NHC-Ag]⁺ fragment that denotes the molecular structure of type erNHC-AgX which could be further confirmed by X-ray diffraction analysis of selected examples (Figures 6 and 9).

Next, the synthesis of Cu^I erNHC complexes, following literature protocols, was explored (Scheme 1). For example, by attempting the condensation of erNHC salts and a Cu^I source (i.e. Cu⁰/air, Cu₂O, CuBr),^[25] most starting material was recovered and only traces of byproduct were isolated, presumably formed upon oxidation of the C_{NHC} under heating in open-air conditions (Pathway B). At the latter, the synthesis of Cu^I erNHC complexes was accomplished by the free carbene strategy, involving the in situ deprotonation of the erNHC salts (**1 a**) in presence of (SMe₂)CuBr (Pathway C).^[26]

Gratifyingly, most of the erNHC salts underwent deprotonation under these conditions and complexes **8–15** were successfully obtained (Figure 4). All of the Cu^I erNHC complexes adopt a neutral, mononuclear erNHC-Cu-Br conformation as judged in the ¹H-NMR spectra which remained identical to those of Ag^I erNHC complexes and the previously reported Au^I erNHC ones.^[14]

The carbene carbon signals in the ¹³C{¹H} NMR spectra show a singlet at around $\delta=223$ ppm for the nine-membered NHCs (9-erNHC), and at around $\delta=214$ ppm for the ten-membered NHC (10-erNHC). This implies that the C_{NHC} in the 9-erNHC is significantly less shielded (by ca. δ 9 ppm) than the respective one of the 10-erNHC. In general, the carbenic carbon of Cu^I erNHC complexes is highfield shifted by ca. $\Delta\delta=10$ ppm than their Ag^I erNHC congeners. HRMS spectra (ESI+) of Cu^I erNHC complexes reflect the peak of the [NHC-Cu]⁺ fragment at the highest intensity nevertheless, the [(NHC)₂Cu]⁺ species was also found in a minor ratio.

Interestingly, the mass spectrometry analyses of complexes **11** and **15**, bearing less bulky ligands, namely 9-Xyl and

**Scheme 1.** Synthetic approaches to Cu^I erNHC complexes.**Figure 4.** Synthesized Cu^I complexes 8–15 bearing erNHC ligands.

10-Xyl, exhibit peaks of the $[(\text{erNHC-Cu})_2\text{Br}]^+$ and $[(\text{erNHC-Cu})_2\text{Br}]^+$ fragments, which might suggest that the linear erNHC-Cu-Br complex is in equilibrium with the bromide-bridged $\{[(\text{erNHC})_2\text{Cu}(\mu\text{-Br})]\}[\text{Br}]$ species and the neutral tri-coordinate ($\text{erNHC})_2\text{CuBr}$ (Scheme 2).

The equilibrium is displaced towards the formation of neutral mononuclear Cu^I erNHC complex and to support this hypothesis, the structure of **15** was unequivocally established by single-crystal X-ray analysis (Figure 9, right). Although two molecules were found in the unit cell, no evidence of a metallic Cu...Cu interaction or a bromide-bridged species was observed.

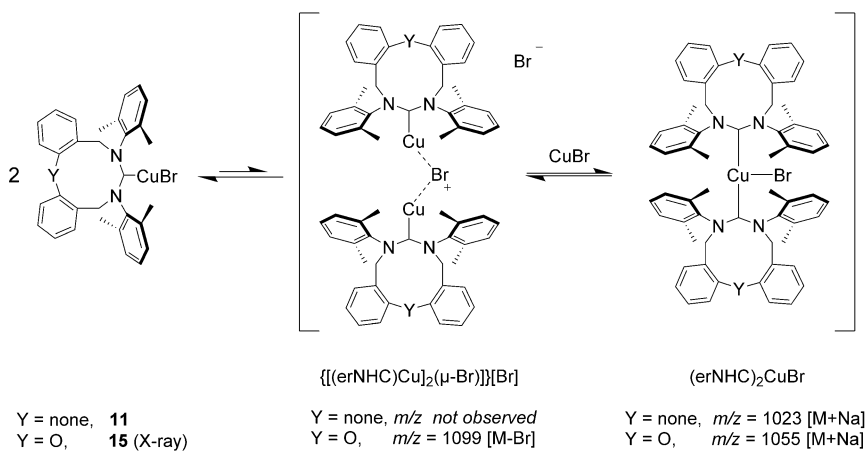
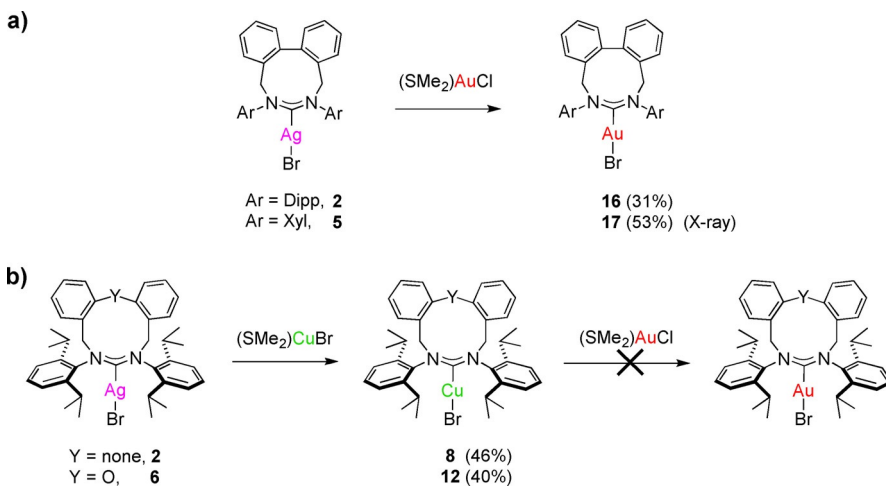
The carbene transfer ability of selected Ag^I compounds in the presence of (SMe₂)AuCl or (SMe₂)CuBr as metal sources was further investigated (Scheme 3). The reaction of **2** or **5** conducted to novel erNHC-AuBr complexes **16** (31% yield) and **17** (53% yield), respectively. These complexes retained the Br⁻ instead of the Cl⁻, contrary to the stability of the insoluble

halide salts which increases in the order AgCl < AgBr < AgI and precipitation of AgBr is more favorable than that of AgCl.^[25] The structure of complex (9-Xyl)AuBr **17** was confirmed by X-ray diffraction analysis of a single crystal (Figure 5).^[22]

By employing the complexes **2** and **6** bearing Dipp ligands, in the presence of (SMe₂)CuBr, the expected Cu^I compounds **8** and **12** were obtained in acceptable yields (40–46%).

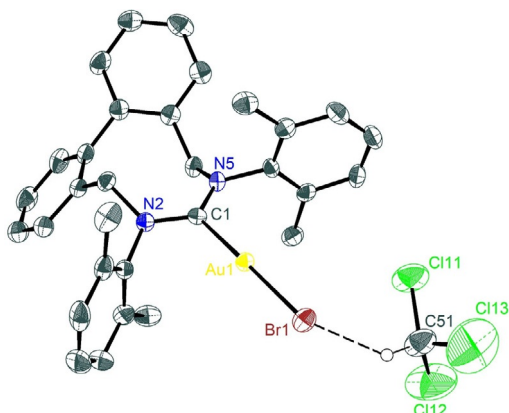
These results underline the carbene transfer ability of the bulky Ag^I erNHC complexes, in contrast to other sterically demanding NHC systems which were unsuccessful in the transfer of ligand to other metals.^[27]

Finally, the Cu^I erNHC complexes **8** and **12** were mixed with (SMe₂)AuCl in the typical conditions for the transfer of ligand (CH₂Cl₂, r.t, light exclusion)^[28] nonetheless, the reaction failed to afford the desired Au^I erNHC complexes and led to the deposition of a gold mirror.

Scheme 2. Postulated equilibrium in solution of Cu^I complexes stabilized by 9-Xyl and 10-Xyl ligands.Scheme 3. Ligand transfer from Ag^I erNHC complexes to (a) Gold and (b) Copper. Reaction conditions: Ag^I complex (0.1 mmol), (SM₂)AuCl or (SM₂)CuBr (0.11 mmol, 1.1 equiv), CH₂Cl₂ (10 mL), room temperature, 24 h, light exclusion.

Structural studies and steric parameters

A single crystal of complex **17**^[22] was grown from a CHCl₃/pentane mixture. This complex crystallized with a CHCl₃ molecule from the solvent (Figure 5).

Figure 5. Molecular structure of (9-Xyl)AuBr·CHCl₃ 17 in the solid state. Thermal ellipsoids are drawn at 50% probability level. Hydrogen atoms are omitted for clarity.

Comparatively, the Au–Br bond length (2.4036(5) Å) is longer than that of Au–Cl found in 9-NHC–Au^I complexes (2.29–2.35 Å).^[14] The C_{NHC}–Au length is 2.006(4) Å and the N–C_{NHC}–N is 119.6(4)°.

X-ray quality single crystals of complexes **2**, **4**, **6**, **7**, **8**, **13** and **15**^[22] were grown by slow diffusion of pentane into a saturated solution of the complex in CH₂Cl₂ or CHCl₃ followed by evaporation of solvents at room temperature. Table 2 summarizes relevant geometrical parameters of Ag^I erNHC complexes **2**, **4**, **6** and **7**, and other related examples selected from literature.

Focusing on the 9-NHCs **2** and **4**, the C_{NHC}–Ag bond lengths are 2.110(4) Å and 2.119(3) Å, respectively. Bond lengths Ag–Br lie between 2.43–2.44 Å and are within the range of the previously reported Ag^I NHC complexes of small ring size (2.38–2.57 Å) but slightly larger than those of the corresponding five-membered compounds (2.11–2.32 Å). The N–C_{NHC}–N angles (118.2–119.1°) are smaller than those of the eight-membered NHCs (123.2–123.3°), and similar to the six- and seven-membered NHCs (6-Mes)AgCl, (6-Dipp)AgBr and (7-Mes)AgBr (118.3–118.9°). C_{NHC}–Cu and Cu–Br bond lengths in Cu^I complex **8** are 1.904(4) Å and 2.2300(8) Å, respectively (Figure 7).

Table 2. Selected geometrical parameters [Å] and [°] and [% V_{bur}]^[29] of some NHC–Ag⁺ complexes.

| Complex | $C_{\text{NHC}}-\text{Ag}$ | Ag–X | $\angle N-C_{\text{NHC}}-\text{N}$ | % V_{bur} |
|-----------------------------------|----------------------------|------------|------------------------------------|--------------------|
| (6-Mes)AgCl ^[18a] | 2.095(3) | 2.3213(1) | 118.3(3) | 44.0 |
| (6-Dipp)AgBr ^[18b, 5e] | 2.104(6) | 2.4254(9) | 118.8(5) | 49.5 |
| (7-Mes)AgI ^[5e] | 2.097(6) | 2.3792(2) | 118.8(6) | 44.7 |
| (7-Xyl)AgI ^[5e] | 2.114(6) | 2.5659(7) | 121.2(5) | 43.6 |
| (IPent)AgOAc ^[16d] | 2.067(1) | 2.111(2) | 103.9(6) | 48.6 |
| (8-Mes)AgBr ^[8a] | 2.132(4) | 2.4553(5) | 123.2(3) | 48.7 |
| (8-Xyl)AgBr ^[8a] | 2.123(3) | 2.4370(5) | 123.3(3) | 49.1 |
| (10-Dietph)AgBr 7 | 2.135(7) | 2.4285(10) | 126.6(7) | 50.3 |
| (9-Dipp)AgBr 2 | 2.110(4) | 2.4314(5) | 118.1(3) | 51.9 |
| (9-Dietph)AgBr 4 | 2.119(3) | 2.4399(5) | 119.1(3) | 53.3 |
| (IPr*)AgCl ^[27a] | 2.081(2) | 2.3189(9) | 104.2(2) | 53.5 |
| (10-Dipp)AgBr 6 | 2.137(3) | 2.4449(4) | 126.5(3) | 56.6 |
| (IPr*(2-Np))AgCl ^[12h] | 2.068(2) | 2.317(14) | 104.2(1) | 57.4 |

The $N-C_{\text{NHC}}-\text{N}$ angle found in **8** is 119.0° . Complexes **2** and **4** adopted nearly linear erNHC–Ag–Br geometry with $C_{\text{NHC}}-\text{Ag}-\text{Br}$ angles around 176° while complex **8** appeared considerably out of linearity ($\angle C_{\text{NHC}}-\text{Cu}-\text{Br}=174.7(15)^\circ$).

The torsion angles (α°) found in these complexes are 48.4° , 37.9° and 28.4° , respectively.^[30] The latter values confirm the twisting of the aryls, with respect to the NHC plane, observed in the solid-state structures of the complexes (see (a) in Figure 8). While a sharp twisting is perceived in Ag⁺ complex **2** (top, Figure 6; $\alpha=48.4^\circ$), a significantly smaller twisting is observed in the isostructural Cu⁺ congener **8** (Figure 7, $\alpha=28.4^\circ$).

Moving to the X-ray structures of the 10-erNHC complexes of Ag⁺ and Cu⁺ from a front view (top, Figure 9), is easy to disclose their wide $N-C_{\text{NHC}}-\text{N}$ angles ($126\text{--}128^\circ$). Cu⁺ complex **13** exhibit the widest $N-C_{\text{NHC}}-\text{N}$ angle of this series (128.6°) followed by complexes **6**, **7** and **15** (around 126°). To the best of our knowledge these are the widest $N-C_{\text{NHC}}-\text{N}$ angles of any erNHC–metal complex in current literature. $C_{\text{NHC}}-\text{Ag}$ bond lengths of **6** and **7** lie around 2.14 \AA and are marginally longer than those of six- to eight-membered NHCs, while the Ag–X bond distances are within the same range $2.42\text{--}2.44\text{ \AA}$ (Table 2).

The $C_{\text{NHC}}-\text{Cu}$ bond distances found in Cu⁺ complexes **13** and **15** are $1.924(12)\text{ \AA}$ and $1.915(4)\text{ \AA}$, respectively. To our surprise, torsion angles of these 10-erNHC complexes lie between 0° and 4.5° , which implies that the two aryl planes are essentially in coplanarity with the NHC plane.

This implies that the geometry of the diphenylether moiety exerts a *domino effect* in the overall arrangement of the erNHC complex, which ends up in diminished torsions of the *N*-Aryls. The folding (see (b) in Figure 8) of the diphenylether moiety influences the arrangement of the methylene groups, which adopt a nearly tetrahedral arrangement with $N-\text{CH}_2-\text{C}_\text{Ar}$ angles $b=112.7\text{--}118.9^\circ$ (see (c) in Figure 8). Along with the non-trivial presence of hydrogen atoms in these methylene groups, the folding limit the twisting of the *N*-Aryls as their *ortho*-substituents are equally pushed down and consequently, the *N*-aryl planes reach the more stable geometry (the coplanarity relative to the NHC plane). The molecular structures from side-views presented in Figure S1 showcase the folding of the back-

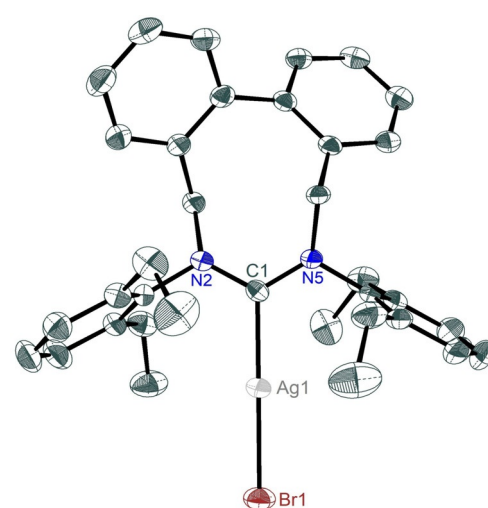
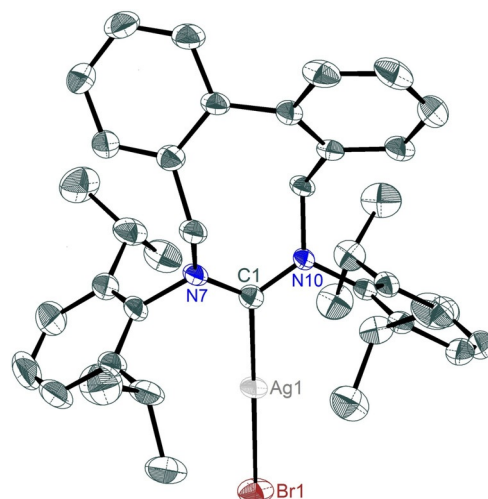


Figure 6. Molecular structures of (9-Dipp)AgBr (**2**, top) and (9-Dietph)AgBr (**4**, bottom) in the solid state. Thermal ellipsoids are drawn at 50% probability level. Hydrogen atoms are omitted for clarity. For **4** only one of the two symmetry-independent molecules is shown.

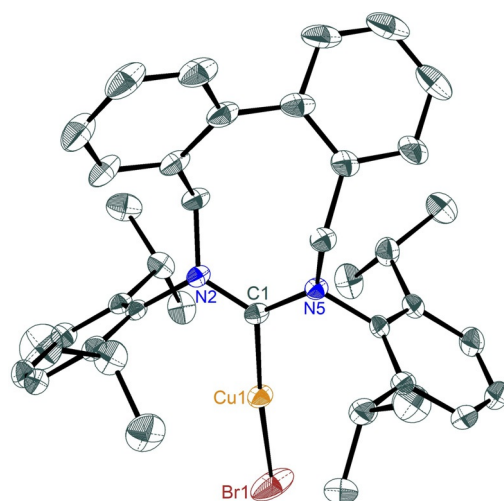


Figure 7. Solid state molecular structure of (9-Dipp)CuBr (**8**). Thermal ellipsoids are drawn at 50% probability level. Hydrogen atoms and one CH_2Cl_2 solvent molecule are omitted for clarity.

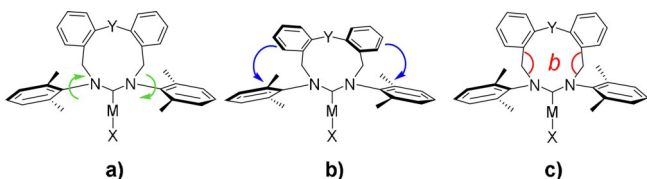


Figure 8. Didactic illustration of (a) the twisting of the *N*-Aryls around the *N*...*N* co-planarity, (b) the folding of the backbone ring limiting the twisting of the *ortho*-substituents at the *N*-Aryls, and (c) the angles *b* defined by $N\text{-CH}_2\text{-CAr}$.

bone ring and the twisting of the *N*-aryls (see Supporting Information).

For the quantification of the steric profiles of Ag^+ and Cu^+ erNHC complexes, the buried volume values ($\%V_{\text{bur}}$)^[29] and topographic steric maps^[31] were derived using SambVca 2.0 package.^[32] The typical settings for the calculation ($r=3.5 \text{ \AA}$ (radius of the sphere around the metal center), $d=2.0 \text{ \AA}$ (bond length $C_{\text{NHC}}\text{-metal}$), Bondi radii scaled by 1.17 and a mesh spacing of 0.10 \AA) were used to scan the sphere of the buried voxels.^[33] The steric distribution around the first coordination sphere of the metal (upper hemisphere), is represented by iso-contour lines visualized from a bottom point. In addition, the colour scale help to identify the less-to-more buried (occupied) zones. Figure 10, features illustrations that resemble the coordination sphere in whose center the metal lies (Ag or Cu) and the reference axes (X , Y) partition the hemisphere, giving the steric component for each quadrant.

The $\%V_{\text{bur}}$ values of Ag^+ erNHC complexes given in the Table 2, are in the range 50.3–56.6% and are comparatively higher than those of the six- to eight-membered NHCs coun-

terparts ($\%V_{\text{bur}}$ up to 49.5). Noteworthy, Ag^+ complex **6** surpass the $\%V_{\text{bur}}$ value of the extremely hindered (*iPr** AgCl complex reported by Markó *et. al.*, ($\%V_{\text{bur}}=53.5$)^[27a] and beside to (*iPr** AgCl ($\%V_{\text{bur}}=57.4$),^[12h] these represent the structurally more imposing NHC– Ag^+ complexes in current literature.

The steric maps of the 10-erNHC complexes are presented in Figure 9 (bottom). In complex **6** ($\%V_{\text{bur}}=56.6$), the *ortho*-isopropyl substituents of the *N*2- and *N*5-Aryl substituents prevent the rotation around the *N*-Aryl bond effectively, by limiting the twisting of the Dipp substituents, which results in a homogeneous steric delivery. Although the top-left quadrant is less bulky (46.4%), the steric impact of the ligand lies on the three bulkier quadrants (59–63% buried volume). Similarly, complex **7** ($\%V_{\text{bur}}=50.3$) two quadrants exert lower steric impact (42–45%) than the top-left quadrant which overcomes 60% buried volume.

The $\%V_{\text{bur}}$ value calculated for Cu^+ complex **13** (52.1%), is marginally larger than that of **15** (51.9%) as their structures differ only in the presence of *para*-methyl groups at the *N*-aryls. The torsion angles (0° and 3.3° , respectively), best describe a slight, but still relevant influence of these *para*-methyl substituents, into the steric distribution of the complex, through the stabilization of the NHC skeleton. We might better illustrate this with the imprint of one *para*-methyl substituent visible in the steric map of **13** (see the blue area), whereas in analogous zone of **15**, there is no trace of covered field as its *para* position is vacant (Figure 9).

Since a direct comparison between two NHC complexes possessing different metals might be meaningless,^[7e] a few interesting observations, regarding the steric impact of 9-Dipp

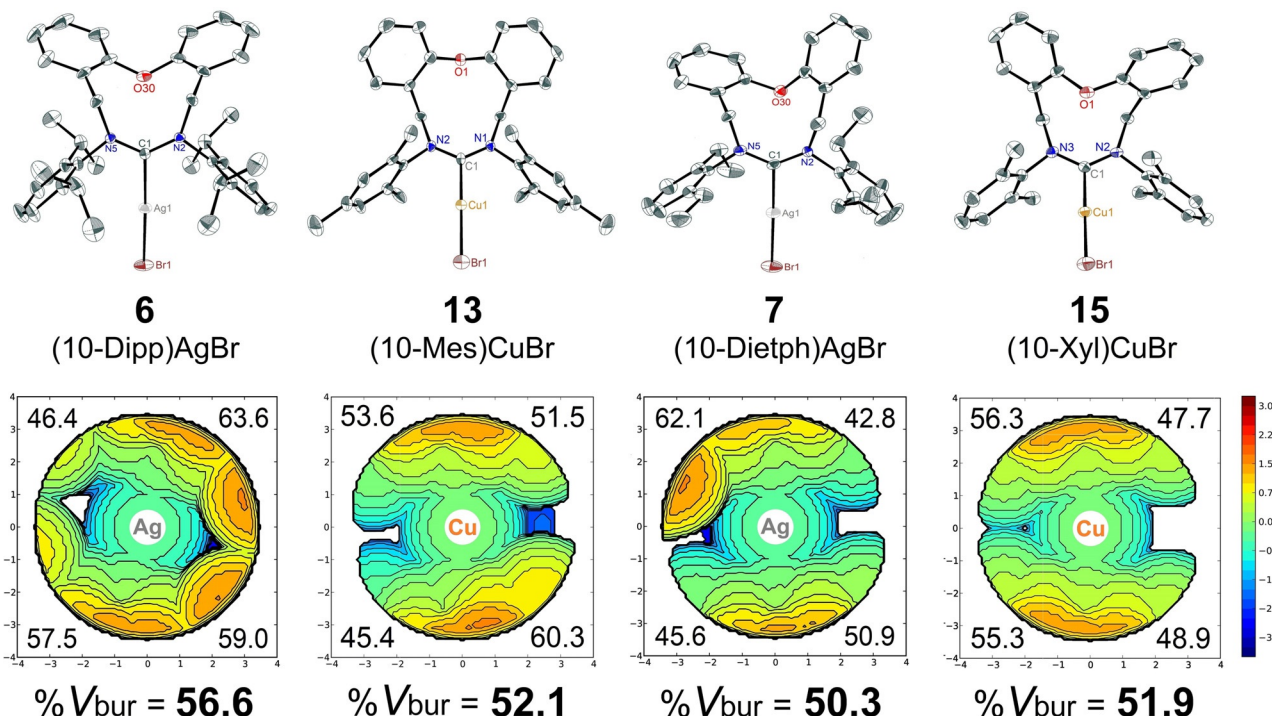


Figure 9. Top (left to right): Solid state molecular structures of (10-Dipp)AgBr (**6**), (10-Mes)CuBr (**13**), (10-Dietph)AgBr (**7**), and (10-Xyl)CuBr (**15**) in the solid state. Ellipsoids drawn at 50% probability level. Solvent molecules and hydrogen atoms have been omitted for clarity. Bottom (left to right): Steric maps of (10-Dipp)AgBr (**6**), (10-Mes)CuBr (**13**), (10-Dietph)AgBr (**7**), and (10-Xyl)CuBr (**15**). Values in the four corners of the maps are the $\%V_{\text{bur}}$ of the erNHC ligand in the corresponding quadrant. The positive values (in \AA) refer to the upper hemisphere, which is the hemisphere where the NHC ligand dwells.

ligand on these erNHC complexes can be pointed out. The steric maps of Ag⁺ complex **2** and Cu⁺ complex **8**, are shown in Figure 10. The steric contribution of the 9-Dipp ligand in Cu⁺ complex **8** (bottom) is notably higher than that of its Ag⁺ congener **2** (top). The top-left quadrant of **2** (45.3%) is less hindered than the analogous quadrant of **8** (55.4%) and a similar asymmetry can be appreciated in the corresponding right tail quadrants (51.1% and 59.1%, respectively). The overall buried volume of complex **2** (51.9%) is still outstanding within the family of Ag⁺ erNHC complexes, while complex **8**, possess the most sterically encumbered structure within the Cu⁺ erNHC family, displaying an impressive %V_{bur}=57.5%.

The size of the metal ion and somehow, the halogen size, are also factors governing the spatial arrangement of the ligand around the metal itself. Given that the ionic radius of Cu⁺ is just much smaller than that of Ag⁺, the large silver ion may affect the steric distribution by pushing the substituents away from the first coordination sphere, causing a diminished %V_{bur} value.

Catalytic applications of NHC–MX complexes

Our previous study on Au⁺ erNHC complexes, shed light upon the strong effect that the steric distribution of the erNHC complex exerts on the catalyst performance.^[14] For example, we found that (9-Mes)AuCl (%V_{bur}=43.6, $\alpha=39.3^\circ$), promoted the cyclization of a propargylamide in 60% yield (0.025 mol% catalyst loading, 50 °C, 24 h), while (9-Dipp)AuCl (%V_{bur}=53.0, $\alpha=$

48.2°) was not that effective (6% yield) under same reaction conditions. We chose, namely (9-Dipp)CuBr **8** (%V_{bur}=57.5), because it is the bulkiest NHC Cu⁺ complex, in combination with its well-distributed steric demand ($\alpha=28.4^\circ$) as discussed above. To further compliment this preliminary catalytic study, we selected the 10-erNHC complex **12** as it also bears the bulky 9-Dipp ligand. The coupling between *N*-tosylhydrazones and terminal alkynes for the synthesis of Benzofurans was investigated as test reaction (Table 3).^[34]

At 2.5 mol% catalyst loading, both complexes **8** (93% yield) and **12** (88% yield), proved capable of bringing about the coupling between a *N*-tosylhydrazone and phenylacetylene to form benzofuran **3a** after 12 h (Table 3, Entries 1 and 2). Lowering (1.25 mol%) the catalyst loading, complex **8** afforded 68% yield (Entry 3) and an acceptable 41% yield when a 0.5 mol% loading was employed (Entry 4). At 0.25–0.05 mol% loadings (Entries 5 and 6), we observed a poor advance in the reaction (5–22% yield) after 24 h. From the outset, Cu⁺ catalyst **8** showed good result at 0.25 mol% loading, forging the coupling (22% yield, Entry 5) in spite of longer reaction time (24 h). In general, the contribution of the erNHC ligand to the stabilization of the active Cu⁺ species is reflected by the ability of the catalysts to even operate at elevated temperature (100 °C), then complexes **8** and **12** proved their catalytic efficiency (up to 93% yield, 2.5 mol% loading).^[34] The nature of the used NHC ligand is also critical. The replacement of the semi rigid biphenyl moiety in (9-Dipp) ligand by a yet flexible diphenyl ether moiety in (10-Dipp) ligand led to a diminished performance at low loadings (0.50 mol%): the coupling catalyzed by **12** gave only 34% product after 2 days.

We next set about assessing the reach of the catalytic activity of novel erNHC–AuBr complex **16** in the cycloisomerization of *N*-propargylamide **I** (Scheme 4, top).^[35] The reaction was promoted by the gold pre-catalyst (2 mol% loading), and AgNTf₂ as bromide scavenger. Oxazoline **II** was obtained (93% yield) as the only product after 8 h, conducting the reaction in

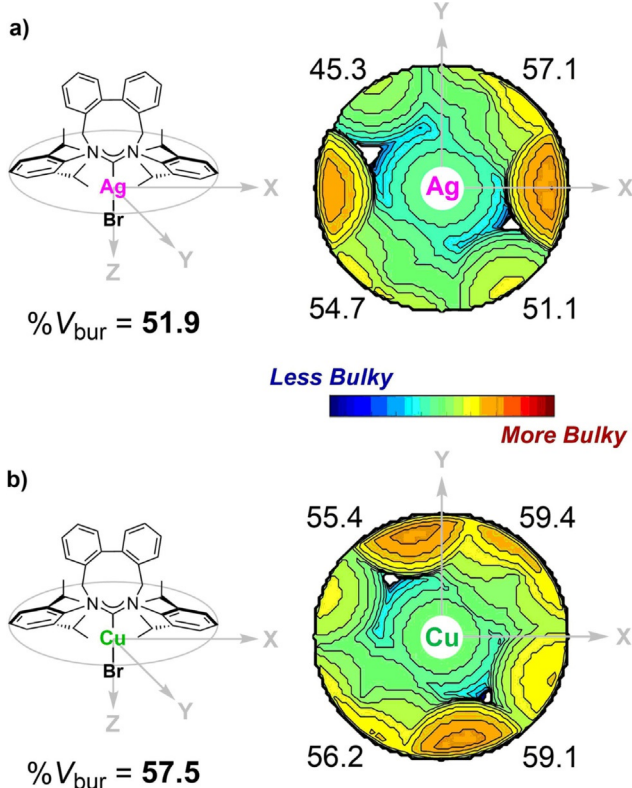


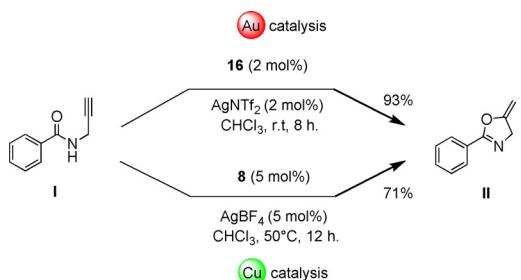
Figure 10. Visualizing of the steric impact of the top hemisphere of **2** (a) and **8** (b) indicating the buried volume for each quadrant.

Table 3. Synthesis of benzofuran **3a** by coupling between 2-hydroxy-*N*-tosylhydrazone and phenylacetylene by using **8** and **12** as catalysts.^[a]

| Entry | [Cu] cat. | [Cu] [mol %] ^[b] | Time [h] | Yield [%] ^[c] | 2a | 3a |
|-------|-----------|-----------------------------|----------|--------------------------|--|--|
| | | | | | Reaction conditions: <i>N</i> -tosylhydrazone (0.10 mmol), phenylacetylene (0.125 mmol), Cs ₂ CO ₃ (0.3 mmol), CH ₃ CN (2.0 mL), 100 °C, sealed tube. | Reaction conditions: <i>N</i> -tosylhydrazone (0.10 mmol), phenylacetylene (0.125 mmol), Cs ₂ CO ₃ (0.3 mmol), CH ₃ CN (2.0 mL), 100 °C, sealed tube. |
| 1 | 8 | 2.5 | 12 | 93 ^[d] | | |
| 2 | 12 | 2.5 | 12 | 88 ^[d] | | |
| 3 | 8 | 1.25 | 12 | 68 ^[d] | | |
| 4 | 8 | 0.50 | 12 | 41 | | |
| 5 | 8 | 0.25 | 24 | 22 | | |
| 6 | 8 | 0.05 | 24 | 5 | | |
| 7 | 12 | 1.25 | 24 | 76 ^[d] | | |
| 8 | 12 | 0.50 | 48 | 34 ^[d] | | |

[a] Reaction conditions: *N*-tosylhydrazone (0.10 mmol), phenylacetylene (0.125 mmol), Cs₂CO₃ (0.3 mmol), CH₃CN (2.0 mL), 100 °C, sealed tube.

[b] Based on Cu content and with respect to the alkyne. [c] Yields determined by GC-MS using dodecane as internal standard. [d] Isolated yield after column chromatography.



Scheme 4. Gold(I)- or copper(I)-catalyzed synthesis of oxazoline **II**. Isolated yields are presented.

chloroform at room temperature. A brief survey on the existing literature reveals only a few examples of gold(I) bromide complexes that spans from six- to eight-membered NHC ligands, including their structural and catalytic features.^[8d,36]

In addition to employing gold pre-catalyst **16**, the use of complex **8**, as a source of the cationic Cu¹ species, was also investigated (Scheme 4, bottom).^[37] By using 5 mol% of complex **8** and AgBF₄ as bromide abstractor, the reaction afforded 71% of the expected product **II** after 12 h under heating conditions. A summary of screening experiments for this reaction can be found in Table S1 (see the Supporting Information). The use **8** and AgBF₄ separately, yielded no product under similar conditions, a fact that we interpret as evidence of the cationic moiety (9-Dipp)Cu⁺, either solvated or in contact to BF₄⁻, as the active catalytic species.

Arguably, activity of Cu¹ complex **8**, is likely due to the large steric environment imparted by the 9-Dipp ligand around the metal center, that is able to stabilize the erNHC-Cu⁺ species upon halide abstraction, so that the cycloisomerization of **I** is catalyzed by a π-acidic copper cation and favored by i) the presence of a weakly (BF₄⁻) coordinated anion and ii) the steric stabilization of a erNHC ligand with bulky (Dipp) substituents (complex **8** has the largest calculated %V_{bur} (57.5%) of any NHC-Cu¹ reported to date).

Conclusions

In summary, we succeeded in the synthesis and full characterization of new Ag¹ and Cu¹ complexes with sterically demanding expanded-ring NHC ligands. The steric profiling was made in terms of two fundamental descriptors, the %V_{bur} which revealed the highest value for any erNHC-stabilized complex reported to date (**8**, V_{bur}=57.5%), and the topographic steric maps, that illuminated the real impact of the erNHC ligands in the first coordination sphere of the metal center where the catalysis take place. In contrast to the alky-chain-based erNHC ligands, our analysis indicates that a limited twisting of the N-Aryls, is related to the folded backbone ring and contributes to an improved spatial arrangement of the NHC skeleton by pushing the *ortho*-substituents of the N-Aryls into the metal's coordination sphere. Hence, the effective stabilization of the current Ag¹ and Cu¹ erNHC complexes benefits from the joint effect of the steric demanding nature of the bulky Dipp substituents and the semi-rigid nature of the erNHC backbone.

The present work spotlights the first studies on Cu¹ erNHC complexes as catalysts in coupling and cycloisomerization reactions proving their high efficiency and resilience to heating. The positive outcomes disclose their potential use in π-acid catalysis.

Acknowledgements

A. C. R. is grateful for a Ph.D. fellowship from Consejo Nacional de Ciencia y Tecnología (México).

Conflict of interest

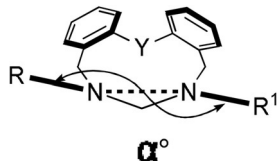
The authors declare no conflict of interest.

Keywords: buried volume • carbene ligands • copper • N-heterocyclic carbenes • silver

- [1] a) H. W. Wanzlick, *Angew. Chem. Int. Ed.* **1962**, *1*, 75–80; *Angew. Chem. 1962*, *74*, 129–134; b) H. J. Schönher, H. W. Wanzlick, *Angew. Chem. Int. Engl. 1968*, *7*, 141–142; *Angew. Chem. 1968*, *80*, 154–154.
- [2] a) A. J. Arduengo, R. L. Harlow, M. Kline, *J. Am. Chem. Soc.* **1991**, *113*, 361–363; b) A. J. Arduengo, J. R. Goerlich, W. J. A. Marshall, *J. Am. Chem. Soc.* **1995**, *117*, 11027.
- [3] a) A. Igau, H. Grutzmacher, A. Baceiredo, G. Bertrand, *J. Am. Chem. Soc.* **1988**, *110*, 6463–6466; b) A. Igau, A. Baceiredo, A. Trinquier, G. Bertrand, *Angew. Chem. Int. Engl.* **1989**, *28*, 621–622; *Angew. Chem.* **1989**, *101*, 617–618; c) G. Gillette, A. Baceiredo, G. Bertrand, *Angew. Chem. Int. Engl.* **1990**, *29*, 1429–1431; *Angew. Chem.* **1990**, *102*, 1486–1488; d) R. Jazza, H. Liang, B. Donnadieu, G. Bertrand, *J. Organomet. Chem.* **2006**, *691*, 3201–3205.
- [4] a) W. A. Herrmann, M. Elison, J. Fisher, C. Köcher, G. R. Artus, *Angew. Chem. Int. Engl.* **1995**, *34*, 2371–2374; *Angew. Chem.* **1995**, *107*, 2602–2605; b) W. A. Herrmann, *Angew. Chem. Int. Ed.* **2002**, *41*, 1290–1309; *Angew. Chem.* **2002**, *114*, 1342–1363.
- [5] a) P. L. Arnold, *Heteroat. Chem. Heteroatom Chem.* **2002**, *13*, 534–539; b) V. César, S. Bellemín-Lapponaz, L. H. Gade, *Chem. Soc. Rev.* **2004**, *33*, 619–636; c) C. M. Cruden, D. P. Allen, *Coord. Chem. Rev.* **2004**, *248*, 2247–2273; d) N. M. Scott, S. P. Nolan, *Eur. J. Inorg. Chem.* **2005**, 1815–1828; e) M. Iglesias, D. J. Beetstra, J. C. Knight, L. L. Ooi, A. Stasch, S. Coles, L. Male, M. B. Hursthouse, K. J. Cavell, A. Dervisi, I. A. Fallis, *Organometallics* **2008**, *27*, 3279–3289; f) S. Díez-González, N. Marion, S. P. Nolan, *Chem. Rev.* **2009**, *109*, 3612–3676; g) D. J. Nelson, S. P. Nolan, *N-heterocyclic Carbenes in N-heterocyclic Carbenes: Effective Tools for Organometallic Synthesis* (Ed.: S. P. Nolan), Wiley-VCH, Weinheim, **2014**, ch. 8, pp. 199–242; h) H. Yoshida, *ACS Catal.* **2016**, *6*, 1799–1811; i) M. N. Hopkinson, C. Richter, M. Schedler, F. Glorius, *Nature* **2014**, *510*, 485–496.
- [6] Selected literature about NHC complexes of Ag¹, Cu¹, and Au¹ see:
a) M. M. Díaz-Reqejo, P. J. Pérez, *J. Organomet. Chem.* **2005**, *690*, 5441–5450; b) I. J. B. Lin, C. S. Vasam, *Coord. Chem. Rev.* **2007**, *251*, 642–670; c) J. C. Y. Lin, R. T. W. Huang, C. S. Lee, A. Bhattacharyya, W. S. Hwang, I. J. B. Lin, *Chem. Rev.* **2009**, *109*, 3561–3598; d) S. P. Nolan, *Acc. Chem. Res.* **2011**, *44*, 91–100; e) S. Gaillard, C. S. J. Cazin, S. P. Nolan, *Acc. Chem. Res.* **2012**, *45*, 778–787; f) L. Batiste, P. Chen, *J. Am. Chem. Soc.* **2014**, *136*, 9296–9307; g) A. Doddi, M. Peters, M. Tamm, *Chem. Rev.* **2019**, *119*, 6994–7112; h) N. Marion, *NHC-Copper, Silver and Gold Complexes in Catalysis, N-Heterocyclic Carbenes: From Laboratory Curiosities to Efficient Synthetic Tools*, (Ed.: S. Diez-Gonzalez), RSC Publishing, Cambridge, **2010**, CH. 11, pp. 317–336; i) T. Wurm, A. M. Asiri, A. S. K. Hashmi, *NHC-Au¹ Complexes: Synthesis Activation, and Application, N-Heterocyclic Carbenes: Effective Tools for Organometallic Synthesis* (Ed.: S. P. Nolan), Wiley-VCH, Weinheim, **2014**, ch. 9, pp. 243–267; j) F. Lazreg, F. Nahra, C. S. J. Cazin, *Coord. Chem. Rev.* **2015**, *48*, 293–294; k) A. S. K. Hashmi, C. Lothschütz, C. Böhling, T. Hengst, C. Hubbert, F. Rominger, *Adv. Synth.*

- Catal.* **2010**, *352*, 3001–3012; l) D. Riedel, T. Wurm, K. Graf, M. Rudolph, F. Rominger, A. S. K. Hashmi, *Adv. Synth. Catal.* **2015**, *357*, 1515–1523; m) A. S. K. Hashmi, C. Lothschütz, K. Graf, T. Häffner, A. Schuster, F. Rominger, *Adv. Synth. Catal.* **2011**, *353*, 1407–1412; n) C. Lothschütz, T. Wurm, A. Zeiler, A. Freiherr v. Falkenhausen, M. Rudolph, F. Rominger, A. S. K. Hashmi, *Chem. Asian J.* **2016**, *11*, 342–346; o) A. S. K. Hashmi, T. Hengst, C. Lothschütz, F. Rominger, *Adv. Synth. Catal.* **2010**, *352*, 1315–1337; p) A. S. K. Hashmi, D. Riedel, M. Rudolph, F. Rominger, T. Oeser, *Chem. Eur. J.* **2012**, *18*, 3827–3830.
- [7] a) L. Cavallo, A. Correa, C. Costabile, H. Jacobsen, *J. Organomet. Chem.* **2005**, *690*, 5407–5413; b) S. Díez-González, S. P. Nolan, *Coord. Chem. Rev.* **2007**, *251*, 874–883; c) S. Würtz, F. Glorius, *Acc. Chem. Res.* **2008**, *41*, 1523–1533; d) H. Clavier, S. P. Nolan, *Chem. Commun.* **2010**, *46*, 841–861; e) A. Gómez-Suárez, D. J. Nelson, S. P. Nolan, *Chem. Commun.* **2017**, *53*, 2650–2660; f) M. C. Jahnke, F. E. Hahn, Introduction to *N-Heterocyclic Carbenes: Synthesis and Stereoelectronic Parameters*, in *N-Heterocyclic Carbenes: From Laboratory Curiosities to Efficient Synthetic Tools*, (Eds.: S. Diez-Gonzalez), RSC Publishing, Cambridge, **2010**, ch. 1, pp. 1–41; g) W. Y. Lu, K. J. Cavell, J. S. Wixey, B. Kariuki, *Organometallics* **2011**, *30*, 5649–5655; h) J. Li, W. X. Shen, X. R. Li, *Curr. Org. Chem.* **2012**, *16*, 2879–2891; i) M. J. Page, W. Y. Lu, R. C. Poulsen, E. Carter, A. G. Algarra, B. M. Kariuki, S. A. Macgregor, M. F. Mahon, K. J. Cavell, D. M. Murphy, M. K. Whittlesey, *Chem. Eur. J.* **2013**, *19*, 2158–2167; j) A. Kumar, D. Yuan, H. V. Huynh, *Inorg. Chem.* **2019**, *58*, 7545–7553.
- [9] a) J. J. Dunsford, K. J. Cavell, *Dalton Trans.* **2011**, *40*, 9131–9135; b) J. J. Dunsford, D. S. Tromp, C. J. Elsevier, K. J. Cavell, B. M. Kariuki, *Dalton Trans.* **2013**, *42*, 7318–7329; c) L. R. Collins, T. M. Rookes, M. F. Mahon, I. M. Riddlestone, M. K. Whittlesey, *Organometallics* **2014**, *33*, 5882–5887; d) J. J. Dunsford, K. J. Cavell, *Organometallics* **2014**, *33*, 2902–2905; e) N. Phillips, T. Dodson, R. Tirfoin, J. I. Bates, S. Aldridge, *Chem. Eur. J.* **2014**, *20*, 16721–16731; f) A. R. Leverett, A. I. McKay, M. L. Cole, *Dalton Trans.* **2015**, *44*, 498–500; g) J. J. Dunsford, D. J. Evans, T. Pugh, S. N. Shah, N. F. Chilton, M. J. Ingleson, *Organometallics* **2016**, *35*, 1098–1106; h) L. Banach, P. A. Guńka, W. Buchowicz, *Dalton Trans.* **2016**, *45*, 8688–8692; i) T. Wurm, F. Mulks, C. R. N. Böhling, D. Riedel, P. Zargaran, M. Rudolph, F. Rominger, A. S. K. Hashmi, *Organometallics* **2016**, *35*, 1070–1078; j) E. Ö. Karaca, M. Akkoç, M. N. Tahir, C. Arıcı, F. İmik, N. Gürbüz, S. Yaşar, I. Özdemir, *Tetrahedron Lett.* **2017**, *58*, 3529–3532; k) E. Ö. Karaca, M. Akkoç, E. Öz, S. Altin, V. Dorcet, T. Roisnel, N. Gürbüz, Ö. Çelik, A. Bayri, C. Bruneau, S. Yaşar, I. Özdemir, *J. Coord. Chem.* **2017**, *70*, 1270–1284; l) K. R. Sampford, J. L. Carden, E. B. Kidner, A. Berry, K. J. Cavell, D. M. Murphy, B. M. Kariuki, P. D. Newman, *Dalton Trans.* **2019**, *48*, 1850–1858.
- [10] a) M. Iglesias, D. J. Beetstra, A. Stasch, P. N. Horton, M. B. Hursthouse, S. J. Coles, K. J. Cavell, A. Dervisi, I. A. Fallis, *Organometallics* **2007**, *26*, 4800–4809; b) C. J. E. Davies, M. J. Page, C. E. Ellul, M. F. Mahona, M. K. Whittlesey, *Chem. Commun.* **2010**, *46*, 5151–5153; c) P. Hauwert, J. J. Dunsford, D. S. Tromp, J. J. Weigand, M. Lutz, K. J. Cavell, C. J. Elsevier, *Organometallics* **2013**, *32*, 131–140; d) Q. Teng, W. Wu, H. A. Duong, H. V. Huynh, *Chem. Commun.* **2018**, *54*, 6044–6047.
- [11] a) A. Binobaid, M. Iglesias, D. J. Beetstra, B. Kariuki, A. Dervisi, I. A. Fallis, K. J. Cavell, *Dalton Trans.* **2009**, 7099–7112; b) J. J. Dunsford, K. J. Cavell, B. Kariuki, *J. Organomet. Chem.* **2011**, *696*, 188–194; c) E. L. Kolychov, A. F. Asachenko, P. B. Dzhevakov, A. A. Bush, V. V. Shuntikov, V. N. Khrustalev, M. S. Nechaev, *Dalton Trans.* **2013**, *42*, 6859–6866; d) O. S. Morozov, A. V. Lunchev, A. A. Bush, A. A. Tukov, A. F. Asachenko, V. N. Khrustalev, S. S. Zalesskiy, V. P. Ananikov, M. S. Nechaev, *Chem. Eur. J.* **2014**, *20*, 6162–6170; e) M. A. Topchiy, P. B. Dzhevakov, M. S. Rubina, O. S. Morozov, A. F. Asachenko, M. S. Nechaev, *Eur. J. Org. Chem.* **2016**, 1908–1914.
- [12] a) L. Jafarpour, E. D. Stevens, S. P. Nolan, *J. Organomet. Chem.* **2000**, *606*, 49–54; b) G. Altenhoff, R. Goddard, C. W. Lehmann, F. Glorius, *J. Am. Chem. Soc.* **2004**, *126*, 15195–15201; c) F. Lavallo, G. D. Frey, B. Donnadeieu, M. Soleilhavoup, G. Bertrand, *Angew. Chem. Int. Ed.* **2008**, *47*, 5224–5228; d) S. Würtz, C. Lohre, R. Fröhlich, K. Bergander, F. Glorius, *J. Am. Chem. Soc.* **2009**, *131*, 8344–8345; e) S. G. Alexander, M. L. Cole, J. C. Morris, *New J. Chem.* **2009**, *33*, 720–724; f) T. Dröge, F. Glorius, *Angew. Chem. Int. Ed.* **2010**, *49*, 6940–6952; g) S. G. Weber, C. Loos, F. Rominger, B. F. Straub, *Archivoc* **2012**, *3*, 226–242; h) S. Dierick, D. F. Dewez, I. E. Markó, *Organometallics* **2014**, *33*, 677–683; i) M. W. Hus- song, W. T. Hoffmeister, F. Rominger, B. F. Straub, *Angew. Chem. Int. Ed.* **2015**, *54*, 10331–10335; j) P. Shaw, A. R. Kennedy, D. J. Nelson, *Dalton Trans.* **2016**, *45*, 11772–11780; k) Y. Tang, I. Benissa, M. Huynh, L. Vendier, N. Lugan, S. Bastin, P. Belmont, V. César, V. Michelet, *Angew. Chem. Int. Ed.* **2019**, *58*, 7977–7981; l) *Angew. Chem.* **2019**, *131*, 8061–8065.
- [13] a) P. Bazinet, G. P. A. Yap, D. S. Richeson, *J. Am. Chem. Soc.* **2003**, *125*, 13314–13315; b) M. Mayr, K. Wurst, K. Ongania, M. R. Buchmeiser, *Chem. Eur. J.* **2004**, *10*, 1256–1266; c) W. A. Herrmann, S. K. Schneider, K. Öfele, M. Sakamoto, E. J. Herdtweck, *J. Organomet. Chem.* **2004**, *689*, 2441–2449; d) C. C. Scarborough, M. J. W. Grady, I. A. Guzei, B. A. Gandhi, E. E. Bunel, S. S. Stahl, *Angew. Chem. Int. Ed.* **2005**, *44*, 5269–5272; e) C. C. Scarborough, B. V. Popp, I. A. Guzei, S. S. Stahl, *J. Organomet. Chem.* **2005**, *690*, 6143–6145; f) M. Wieteck, M. H. Larsen, P. Nösel, J. Schulmeister, F. Rominger, M. Rudolph, M. Pernpointner, A. S. K. Hashmi, *Adv. Synth. Catal.* **2016**, *358*, 1449–1462; g) I. Özdemir, N. Gürbüz, Y. Gök, B. Çetinkaya, *Heteroat. Chem.* **2008**, *19*, 82–86; h) M. Iglesias, D. J. Beetstra, B. Kariuki, K. J. Cavell, A. Dervisi, I. A. Fallis, *Eur. J. Inorg. Chem.* **2009**, 1913–1919; i) J. J. Dunsford, B. M. Kariuki, K. J. Cavell, *Organometallics* **2012**, *31*, 4118–4121; j) L. Huang, Y. Cao, M. Zhao, Z. Tangb, Z. Sun, *Org. Biomol. Chem.* **2014**, *12*, 6554–6556; k) B.-M. Yang, K. Xiang, Y.-Q. Tu, S.-H. Zhang, D.-T. Yang, S.-H. Wang, F.-M. Zhanga, *Chem. Commun.* **2014**, *50*, 7163–7165; l) S. Pelties, E. Carter, A. Folli, M. F. Mahon, D. M. Murphy, M. K. Whittlesey, R. Wolf, *Inorg. Chem.* **2016**, *55*, 11006–11017; m) F. F. Mulks, P. W. Antoni, F. Rominger, A. S. K. Hashmi, *Adv. Synth. Catal.* **2018**, *360*, 1810–1821; n) A. S. K. Hashmi, C. Lothschütz, C. Böhling, F. Rominger, *Organometallics* **2011**, *30*, 2411–2417.
- [14] A. Cervantes-Reyes, F. Rominger, M. Rudolph, A. S. K. Hashmi, *Chem. Eur. J.* **2019**, *25*, 11745–11757.
- [15] a) M. L. Teyssot, A. S. Jarrousse, M. Manin, A. Chevry, S. Roche, F. Norre, C. Beaudoin, L. Morel, D. Boyer, R. Mahiou, A. Gautier, *Dalton Trans.* **2009**, 6894–6902; b) L. Mercs, M. Albrecht, *Chem. Soc. Rev.* **2010**, *39*, 1903–1912; c) S. Roland, C. Jolivalt, T. Cresteil, L. Eloy, P. Bouhours, A. Hequet, V. Mansuy, C. Vanucci, J.-M. Paris, *Chem. Eur. J.* **2011**, *17*, 1442–1446; d) L. Oehninger, R. Rubbiani, I. Ott, *Dalton Trans.* **2013**, *42*, 3269–3284; e) R. Visbal, V. Fernández-Moreira, I. Marzo, A. Laguna, M. C. Gimeno, *Dalton Trans.* **2015**, *44*, 11911–11918.
- [16] a) Y. B. Li, X. F. Chen, Y. Song, L. Fang, G. Zou, *Dalton Trans.* **2011**, *40*, 2046–2052; b) Z. Wang, J. Wen, Q. W. Bi, X. Q. Xu, Z. Q. Shen, X. Y. Li, Z. L. Chen, *Tetrahedron Lett.* **2014**, *55*, 2969–2972; c) K. Yamashita, S. Hase, Y. Kayaki, T. Ikariya, *Org. Lett.* **2015**, *17*, 2334–2337; d) V. H. L. Wong, S. V. C. Vummali, L. Cavallo, A. J. P. White, S. P. Nolan, K. K. Hii, *Chem. Eur. J.* **2016**, *22*, 13320; e) S. Dabral, B. Bayarmagnai, M. Hermens, J. Schießl, V. Mormul, A. S. K. Hashmi, T. Schaub, *Org. Lett.* **2019**, *21*, 1422–1425; f) S. Dabral, U. Licht, P. Rudolf, G. Bollmann, A. S. K. Hashmi, T. Schaub, *Green Chem.* **2020**, doi: 10.1039/C9gc04320a; g) G. Fang, X. Bi, *Silver Complexes in Organic Transformations, Silver Catalysis in Organic Synthesis* (Eds.: C.-J. Li, X. Bi), Wiley-VCH, Weinheim, **2018**, ch. 11, pp. 661–722;
- [17] a) H. M. J. Wang, I. J. B. Lin, *Organometallics* **1998**, *17*, 972–975; b) U. Hintermaier, U. Englert, W. Leitner, *Organometallics* **2011**, *30*, 3726–3731; c) H.-L. Su, L. M. Pérez, L. S.-J. Lee, J. H. Reibenspies, H. S. Bazzi, D. E. Bergbreiter, *Organometallics* **2012**, *31*, 4063–4071; d) E. Caytan, S. Roland, *Organometallics* **2014**, *33*, 2115–2118.
- [18] a) F. F. Mulks, P. W. Antoni, J. H. Gross, J. Graf, F. Rominger, A. S. K. Hashmi, *J. Am. Chem. Soc.* **2019**, *141*, 4687–4695; b) E. L. Kolychov, I. A. Portnyagin, V. V. Shuntikov, V. N. Khrustalev, M. S. Nechaev, *J. Organomet. Chem.* **2009**, *694*, 2454–2462; c) A. Rit, T. Pape, F. E. Hahn, *J. Am. Chem. Soc.* **2010**, *132*, 4572–4573; d) C. Topf, C. Hirtenlehner, U. Monkowius, *J. Organomet. Chem.* **2011**, *696*, 3274–3278; e) A. Rit, T. Pape, A. Hepp, F. E. Hahn, *Organometallics* **2011**, *30*, 334–347.
- [19] a) H. Kaur, F. K. Zinn, E. D. Stevens, S. P. Nolan, *Organometallics* **2004**, *23*, 1157–1160; b) S. Díez-González, A. Correa, L. Cavallo, S. P. Nolan, *Chem. Eur. J.* **2006**, *12*, 7558–7564; c) S. Díez-González, E. D. Stevens, N. M. Scott, J. L. Petersen, S. P. Nolan, *Chem. Eur. J.* **2008**, *14*, 158–168; d) S. Díez-González, S. P. Nolan, *Acc. Chem. Res.* **2008**, *41*, 349–358; e) O. Songis, P. Boulens, C. G. M. Benson, C. S. J. Cazin, *RSC Adv.* **2012**, *2*, 11675–11677; f) B. R. M. Lake, C. E. Willans, *Chem. Eur. J.* **2013**, *19*, 16780–16790; g) J. D. Egbert, C. S. J. Cazin, S. P. Nolan, *Catal. Sci. Technol.* **2013**, *3*, 912–926; h) Y. D. Bidal, F. Lazreg, C. S. J. Cazin, *ACS Catal.*

- [20]** a) K. Matsumoto, N. Matsumoto, A. Ishii, T. Tsukuda, M. Hasegawab, T. Tsubomura, *Dalton Trans.* **2009**, 6795–6801; b) R. Marion, F. Sguerra, F. Di-Meo, E. Sauvageot, J.-F. Lohier, R. Daniellou, J.-L. Renaud, M. Linares, M. Hamel, S. Gaillard, *Inorg. Chem.* **2014**, 53, 9181–9191; c) R. Visbala, M. C. Gimeno, *Chem. Soc. Rev.* **2014**, 43, 3551–3574; d) M. Elie, F. Sguerra, F. Di-Meo, M. D. Weber, R. Marion, A. Grimault, J.-F. Lohier, A. Stallivieri, A. Brosseau, R. B. Pansu, J.-L. Renaud, M. Linares, M. Hamel, R. D. Costa, S. Gaillard, *ACS Appl. Mater. Interfaces* **2016**, 8, 14678–14691; e) V. A. Krylova, P. I. Djurovich, M. T. Whited, M. E. Thompson, *Chem. Commun.* **2010**, 46, 6696–6698; f) F. Lazreg, C. S. J. Cazin, *NHC-Copper Complexes and their Applications, N-heterocyclic Carbenes: Effective Tools for Organometallic Synthesis* (Ed.: S. P. Nolan), Wiley-VCH, Weinheim, **2014**, ch. 8, pp. 199–242.
- [21]** a) A. J. Jordan, C. M. Wyss, J. Bacsa, J. P. Sadighi, *Organometallics* **2016**, 35, 613–616; b) G. A. Chesnokov, M. A. Topchiy, P. B. Dzhevakov, P. S. Gribanov, A. A. Tukov, V. N. Khrustalev, A. F. Asachenkov, N. S. Nechaev, *Dalton Trans.* **2017**, 46, 4331–4345; c) J. W. Hall, D. M. L. Unson, P. Brunel, L. R. Collins, M. K. Cybulski, M. F. Mahon, M. K. Whittlesey, *Organometallics* **2018**, 37, 3102–3110; d) F. Sebest, J. J. Dunsford, M. Adams, J. Pivot, P. D. Newman, S. Diez-Gonzalez, *ChemCatChem* **2018**, 10, 2041–2045; e) M. A. Topchiy, A. A. Ageshina, P. S. Gribanov, S. M. Masoud, T. R. Akmalov, S. E. Nefedov, S. N. Osipov, M. S. Nechaev, A. F. Asachenko, *Eur. J. Org. Chem.* **2019**, 1016–1020; f) J. W. Hall, F. Seeberger, M. F. Mahon, M. K. Whittlesey, *Organometallics* **2020**, 39, 227–233.
- [22]** CCDC 1980967 (**1ba**), 1980968 (**2**), 1980969 (**4**), 1980970 (**1ac'**), 1980971 (**6**), 1980972 (**7**), 1980973 (**8**), 1980974 (**13**), 1980975 (**15**), 1980976 (**17**) contain the supplementary crystallographic data for this paper. These data are provided free of charge by The Cambridge Crystallographic Data Centre.
- [23]** a) J. C. Garrison, W. J. Youngs, *Chem. Rev.* **2005**, 105, 3978–4008; b) P. de Frémont, N. M. Scott, E. D. Stevens, T. Ramnial, O. C. Lightbody, C. L. B. Macdonald, J. A. C. Clyburne, C. D. Abernethy, S. P. Nolan, *Organometallics* **2005**, 24, 6301–6309; c) L. Benhamou, E. Chardon, G. Lavigne, S. Bellemain-Lapponnaz, V. César, *Chem. Rev.* **2011**, 111, 2705–2733.
- [24]** H. V. Huynh in *The Organometallic Chemistry of N-heterocyclic Carbenes*, 1st edition, John Wiley & Sons Ltd, Weinheim, **2017**, chapters 3 and 11, pp. 52–90, and 171–218.
- [25]** a) C. A. Citadelle, E. Le-Nouy, F. Bisaro, A. M. Z. Slawin, C. S. J. Cazin, *Dalton Trans.* **2010**, 39, 4489–4491; b) J. Chun, H. Sol-Lee, I. Gu-Jung, S. Won-Lee, H. Jin-Kim, S. Uk-Son, *Organometallics* **2010**, 29, 1518–1521; c) O. Santoro, A. Collado, A. M. Z. Slawin, S. P. Nolan, C. S. J. Cazin, *Chem. Commun.* **2013**, 49, 10483–10485; d) C. Gibard, H. Ibrahim, A. Gautier, F. Cisnetti, *Organometallics* **2013**, 32, 4279–4283; e) B. Liu, X. Ma, F. Wu, W. Chen, *Dalton Trans.* **2015**, 44, 1836–1844; f) B. Liu, Q. Xia, W. Chen, *Angew. Chem. Int. Ed.* **2009**, 48, 5513–5516; *Angew. Chem.* **2009**, 121, 5621–5624.
- [26]** Commercially available CuBr was initially employed nonetheless, due to its rapid oxidation in air, a low purity greenish solid prevailed, which resulted in poor yields. To overcome this, we purify CuBr by preparing the (SM₂)CuBr complex and employed it as freshly crystallized material.
- [27]** a) G. Berthon-Gelloz, M. A. Siegler, A. L. Spek, B. Tinant, J. N. H. Reek, I. E. Markó, *Dalton Trans.* **2010**, 39, 1444–1446; b) A. Gómez-Suárez, R. S. Ramón, O. Songis, A. M. Z. Slawin, C. S. J. Cazin, S. P. Nolan, *Organometallics* **2011**, 30, 5463–5470.
- [28]** For the use of NHC-Cu^I as ligand transfer reagents see: a) G. Venkatachalam, M. Heckenroth, A. Neels, M. Albrecht, *Helv. Chim. Acta* **2009**, 92, 1034–1045; b) M. R. L. Furst, C. S. J. Cazin, *Chem. Commun.* **2010**, 46, 6924–6925; c) F. Nahra, A. Gómez-Herrera, C. S. J. Cazin, *Dalton Trans.* **2017**, 46, 628–631.
- [29]** A. Poater, F. Ragone, S. Giudice, C. Costabile, R. Dorta, S. P. Nolan, L. Cavallo, *Organometallics* **2008**, 27, 2679–2681.
- [30]** The torsion angle (α°) between the planes, defined by the R–N···N–R¹ atoms (vide infra), is a measurement of the spatial twist and the relative position of R and R¹ substituents, which point into the metal's coordination sphere. The narrower the angle, the closer are the substituents that point into the metal center. See Refs. [5e, 10a, 14].



- [31]** A. Poater, F. Ragone, R. Mariz, R. Dorta, L. Cavallo, *Chem. Eur. J.* **2010**, 16, 14348–14353.
- [32]** a) A. Poater, B. Cosenza, A. Correa, S. Giudice, F. Ragone, V. Scarano, L. Cavallo, *Eur. J. Inorg. Chem.* **2009**, 1759–1766; b) L. Falivene, R. Credendino, A. Poater, A. Petta, L. Serra, R. Oliva, V. Scarano, L. Cavallo, *Organometallics* **2016**, 35, 2286–2293.
- [33]** a) F. Ragone, A. Poater, L. Cavallo, *J. Am. Chem. Soc.* **2010**, 132, 4249–4258; b) hydrogen atoms were omitted for the calculation. For direct comparison, listed parameters are identical to those of the NHC examples reported in literature.
- [34]** a) L. Zhou, Y. Shi, Q. Xiao, Y. Liu, F. Ye, Y. Zhang, J. Wang, *Org. Lett.* **2011**, 13, 968–971; b) R. Manzano, T. Wurm, F. Rominger, A. S. K. Hashmi, *Chem. Eur. J.* **2014**, 20, 6844–6848.
- [35]** a) J. P. Weyrauch, A. S. K. Hashmi, A. Schuster, T. Hengst, S. Schetter, A. Littmann, M. Rudolph, M. Hamzic, J. Visus, F. Rominger, W. Frey, J. W. Bats, *Chem. Eur. J.* **2010**, 16, 956–963; compare also: b) A. S. K. Hashmi, M. C. Blanco Jaimes, A. M. Schuster, F. Rominger, *J. Org. Chem.* **2012**, 77, 6394–6408; c) A. S. K. Hashmi, A. Littmann, *Chem. Asian J.* **2012**, 7, 1435–1442; d) A. S. K. Hashmi, M. Rudolph, S. Schymura, J. Visus, W. Frey, *Eur. J. Org. Chem.* **2006**, 4905–4909; A. S. K. Hashmi, J. P. Weyrauch, W. Frey, J. W. Bats, *Org. Lett.* **2004**, 6, 4391–4394.
- [36]** A. Kumar, C. Singh, H. Tinnermann, H. V. Huynh, *Organometallics* **2020**, 39, 172–181.
- [37]** For cationic NHC-Cu^I complexes as catalysts see: a) M. R. Fructos, P. de Frémont, S. P. Nolan, M. M. Díaz-Requejo, P. J. Pérez, *Organometallics* **2006**, 25, 2237–2241; b) S. Díez-González, N. M. Scott, S. P. Nolan, *Organometallics* **2006**, 25, 2355–2358; c) J. Liu, R. Zhang, S. Wang, W. Sun, C. Xia, *Org. Lett.* **2009**, 11, 1321–1324; d) L.-J. Cheng, C. J. Cordier, *Angew. Chem. Int. Ed.* **2015**, 54, 13734–13738; *Angew. Chem.* **2015**, 127, 13938–13942; e) I. Nakamura, T. Jo, Y. Ishida, H. Tashiro, M. Terada, *Org. Lett.* **2017**, 19, 3059–3062; f) Y. Ishida, I. Nakamura, M. Terada, *J. Am. Chem. Soc.* **2018**, 140, 8629–8633.

Manuscript received: February 4, 2020

Revised manuscript received: February 27, 2020

Accepted manuscript online: February 27, 2020

Version of record online: April 20, 2020